Intracellular mechanisms of molecular recognition and sorting for transport of large extracellular matrix molecules

Yoshihiro Ishikawa[a,b], Shinya Ito[c], Kazuhiro Nagata[c], Lynn Y. Sakai[a,b], and Hans Peter Bächinger[a,b,1]

[a]Research Department, Shriners Hospital for Children, Portland, OR 97239; [b]Department of Biochemistry and Molecular Biology, Oregon Health & Science University, Portland, OR 97239; and [c]Department of Molecular Biosciences, Faculty of Life Sciences, Kyoto Sangyo University, Kyoto 603-8555, Japan

Edited by Darwin J. Prockop, Texas A&M Health Science Center, Temple, TX, and approved August 23, 2016 (received for review June 15, 2016)

Extracellular matrix (ECM) proteins are biosynthesized in the rough endoplasmic reticulum (rER) and transported via the Golgi apparatus to the extracellular space. The coat protein complex II (COPII) transport vesicles are approximately 60–90 nm in diameter. However, several ECM molecules are much larger, up to several hundreds of nanometers. Therefore, special COPII vesicles are required to coat and transport these molecules. Transmembrane Protein Transport and Golgi Organization 1 (TANGO1) facilitates loading of collagens into special vesicles. The Src homology 3 (SH3) domain of TANGO1 was proposed to recognize collagen molecules, but how the SH3 domain recognizes various types of collagen is not understood. Moreover, how are large noncollagenous ECM molecules transported from the rER to the Golgi? Here we identify heat shock protein (Hsp) 47 as a guide molecule directing collagens to special vesicles by interacting with the SH3 domain of TANGO1. We also consider whether the collagen secretory model applies to other large ECM molecules.

collagen | secretion | COPII vesicles | Hsp47 | TANGO1

Extracellular matrix (ECM) proteins are the most abundant proteins in our body. They build the body architecture and help to maintain tissue homeostasis in bone, skin, cartilage, and tendon (1). They are biosynthesized in the rough endoplasmic reticulum (ER; rER) and traverse the Golgi apparatus en route to the extracellular space. A transport vesicle for cargo exists to traffic molecules from the rER into the extracellular space. This secretory vesicle is called a coat protein complex II (COPII) vesicle (2–4). It is generated at the ER exit site and usually has a diameter of 60–90 nm. This carrier can transport many secreted proteins. However, larger or elongated molecules, especially collagens and other ECM molecules, will not fit into such small vesicles.

There are more than 20 different collagen types in humans (5, 6). Type I, II, III, and V collagens are classified as fibrillar collagens, which are the most abundant. Type IV collagen is an important structural element in basement membranes. Type VII collagen forms anchoring fibrils at the epidermal–dermal junction in skin. These collagens are all more than 300 nm long. In addition to its elongated triple helical structure, type VII collagen has a 140-kDa noncollagenous domain at the amino terminus. Although more flexible than collagens, fibrillin molecules are also elongated, measured to be approximately 150 nm in length (7). For these molecules, special COPII vesicles or other trafficking systems are required for secretion.

It has been proposed that procollagen molecules, which are the precursors of collagen, are transferred in COPII vesicles to the Golgi (8–10). In 2009, Transmembrane Protein Transport and Golgi Organization 1 (TANGO1), encoded by *MIA3*, was shown to facilitate collagens into COPII vesicles at the ER exit site (11). In the cytoplasm, TANGO1 interacts with Sec23A/Sec24C, the outer molecules of COPII vesicles, and cTAGE5, a homolog of TANGO1 that lacks the rER domains of TANGO. These interactions occur via a proline-rich domain and the second coiled-coil domain, respectively (11, 12). After this report, several molecules, such as Sedlin, Cullin3, and KLHL12 (13, 14), were also identified as being involved in the creation of larger COPII vesicles. Recently t-SNAREs and ER Golgi Intermediate Compartment membranes were involved in "mega-carriers" for type VII procollagen secretion (15, 16).

The TANGO1 KO mouse displayed a severe defect in chondrocyte maturation and bone mineralization in embryos, resulting in dwarfism, peripheral edema, and neonatal lethality (17). Secretion of type I, II, III, IV, VII, and IX collagens was compromised in TANGO1 KO chondrocytes, fibroblasts, endothelial cells, and mural cells. Therefore, TANGO1 clearly plays an important role in collagen trafficking.

A special COPII vesicle for collagens and other large ECM proteins should be synchronized between the rER and the cytoplasm. The Src homology 3 (SH3) domain of TANGO1, located on the inside of the rER, was suggested to recognize type VII collagen (11) and could synchronize collagen synthesis with transport. SH3 domains are generally thought to mediate protein–protein interactions related to intracellular signaling or regulation of cell growth or catalytic activity of proteins (18, 19). The minimal consensus target sequence P*XX*P for SH3 domain binding was defined by early studies, but currently nonconsensus SH3 ligands were also reported (19). The SH3 domain of TANGO1 is a small 7.4-kDa domain composed of 63 aa (residues 45–107 from first methionine; UniProt ID code Q5JRA6). It is not clear how the SH3 domain of TANGO1 can recognize all collagens, as collagens are composed of diverse sequences and also can be homo- or hetero-trimeric triple helices. Moreover, it is not clear whether the SH3 domain can synchronize synthesis and transport of other large ECM proteins.

We demonstrate here that an heat shock protein (Hsp) 47–SH3 domain of TANGO1 complex is required for procollagen trafficking and direction of procollagens toward special transport vesicles. This complex formation solves the important question of how TANGO1 can recognize all different types of collagens.

Significance

The discovery of Transmembrane Protein Transport and Golgi Organization 1 (TANGO1) has given insight into how large extracellular molecules like collagens are loaded into special coat protein complex II (COPII) vesicles for transport. However, because there are more than 20 different collagens in humans, it is not clear how TANGO1 recognizes all collagens. In this manuscript, we show that TANGO1 does not directly interact with collagens. We show instead that the Src homology 3 (SH3) domain of TANGO1 interacts with heat shock protein (Hsp) 47, a chaperone that binds to all different types of collagens. We propose a model in which Hsp47 serves as a guide molecule directing collagens to special COPII vesicles.

Author contributions: Y.I. and H.P.B. designed research; Y.I. performed research; S.I., K.N., and L.Y.S. contributed new reagents/analytic tools; Y.I., L.Y.S., and H.P.B. analyzed data; and Y.I., S.I., K.N., L.Y.S., and H.P.B. wrote the paper.

The authors declare no conflict of interest.

This article is a PNAS Direct Submission.

[1]To whom correspondence should be addressed. Email: hpb@shcc.org.

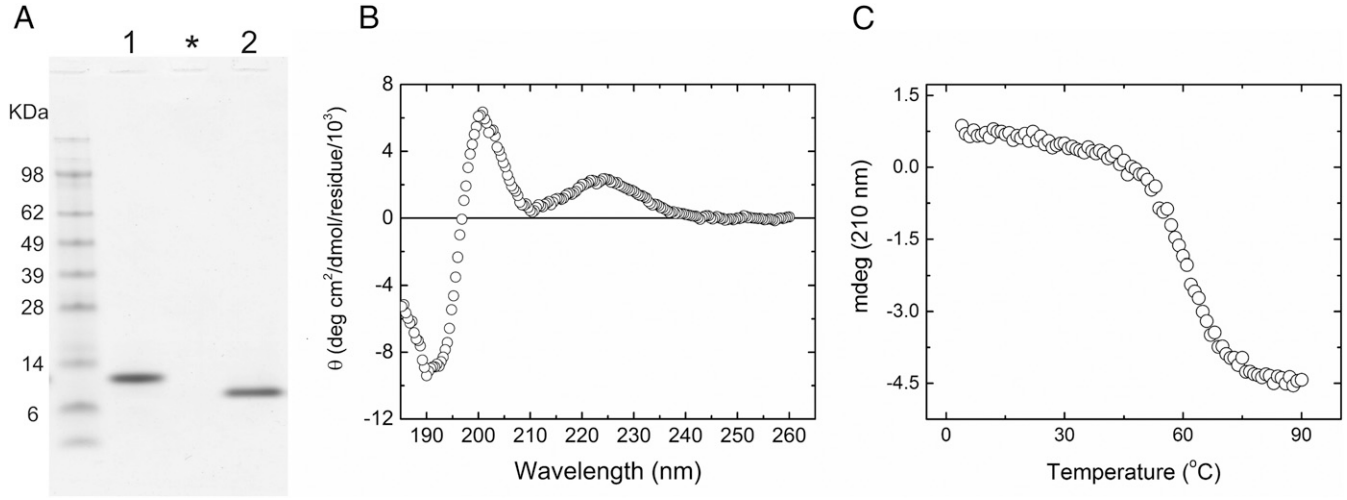

Fig. 1. Characterization of recombinant SH3 domain of human TANGO1. (*A*) SDS/PAGE analysis of purified recombinant SH3 domain of human TANGO1. The SH3 domain was purified from an *E. coli* expression system, and the figure shows the final purified material in the presence and absence of DTT in lanes 1 and 2, respectively. The purified SH3 domain was run on NuPAGE Novex Bis-Tris 4–12% gel (Life Technology) and stained with GelCode Blue Stain Reagent. Asterisk indicates blank lane. (*B*) CD spectra of the SH3 domain. The CD spectrum was measured at 4 °C in 10 mM phosphate, pH 7.5. The concentration of the SH3 domain of human TANGO1 was 8 μM. (*C*) Thermal stability of the SH3 domain of human TANGO1 was monitored by CD at 210 nm, and the rate of heating was 10 °C/h. The concentration of the SH3 domain of human TANGO1 was 8 μM in PBS solution.

Furthermore, we show that this Hsp47–SH3 domain of TANGO1 complex does not recognize other ECM molecules and that, because Hsp47 interacts with fibrillin-1, there may be TANGO1-independent secretory pathways for other large ECM molecules. In addition, our data may indicate that different anchor molecules than Hsp47 for the SH3 domain of TANGO1 may be used for secretion of large molecules like Cartilage Oligomeric Matrix Protein (COMP) or fibronectin, or a TANGO1-independent pathway is also required for these molecules.

Results

The SH3 Domain of Human TANGO1 Barely Recognizes Collagens by Itself. To assess the ability of the SH3 domain of human TANGO1 to recognize collagen molecules directly, we first recombinantly expressed the aminoterminal portion of TANGO1, containing the SH3 domain, in *Escherichia coli*. Fig. 1*A* shows an SDS/polyacrylamide gel of the purified SH3 domain after removal of the His tag in the presence and absence of reducing agent. The purified protein, which consists of Ala-Met-Ala and residues 1–106 of the mature protein, is located below the 14-kDa marker and corresponds well to the expected molecular weight of 12,477 Da. Under nonreducing conditions, it migrates faster than it does under reducing conditions. Four cysteines in the sequence likely form intrachain disulfide bridges, resulting in different migration under reducing and nonreducing conditions. This protein also folds into a stable structure around physiological temperatures, as shown by CD measurements (Fig. 1 *B* and *C*).

To test for direct binding between the SH3 domain of TANGO1 and collagens, surface plasmon resonance (SPR) experiments were performed by using a BIAcore X instrument. The SH3 domain was injected as analyte over the surface of chips, each containing one of eight different types of collagen (type I, II, III, IV, V, VI, X, or XI collagens). Hsp47 was previously shown to bind to native type I, II, III, IV, V, VI, and X collagen by this method (20, 21), and was used as a positive control.

As previously reported, Hsp47 showed direct binding to all types of collagen. In contrast, the SH3 domain only weakly bound to collagens, even though the SH3 domain was used at much higher

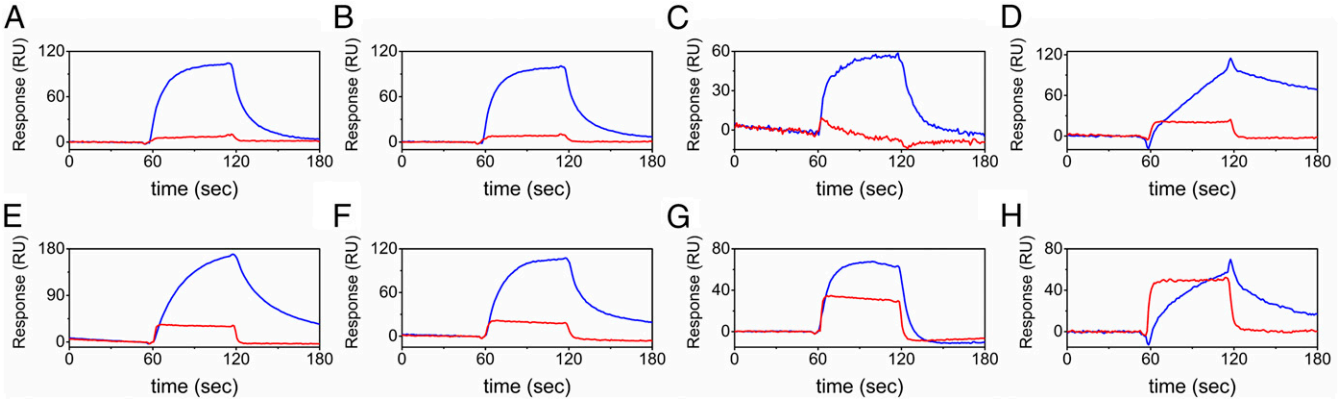

Fig. 2. Direct binding kinetics of the SH3 domain of human TANGO1 to collagens. Direct binding kinetics were measured by SPR analysis using a BIAcore X instrument. The SH3 domain of human TANGO1 (10 μM; red) was injected over CM5 chips immobilized with eight different types of collagen: bovine type I collagen (*A*), bovine type II collagen (*B*), bovine type III collagen (*C*), mouse type IV collagen (*D*), bovine type V collagen (*E*), human type VI collagen (*F*), human recombinant type X collagen (*G*), and bovine type XI collagen (*H*). Hsp47 (0.05 μM; blue) was used as a positive control.

molar concentrations than Hsp47. This weak binding affinity was slightly different for different collagen types (Fig. 2). From these results, we conclude that the SH3 domain barely recognizes collagens by itself.

Hsp47 Is an Anchor Molecule Between the SH3 Domain and Collagens. Results from Fig. 2 show that the SH3 domain by itself is not capable to direct fibrillar collagens into COPII vesicles. Therefore, we hypothesized that an anchor molecule must exist that can recognize collagen triple helices in the rER and can also bind to the SH3 domain of TANGO1. To test this hypothesis, SPR was carried out by using the SH3 domain immobilized to a chip. Three rER molecules recognizing collagen triple helices, FKBP22, FKBP65, and Hsp47, were considered for directing collagens to special COPII vesicles after completion of triple helix formation (22). Hsp47 clearly interacted with the SH3 domain, whereas FKBP22 and FKBP65 did not (Fig. 3*A*), and also showed concentration–dependent binding (Fig. 3*B*). Furthermore, interaction between Hsp47 and the SH3 domain occurred when both binding partners were in solution, as detected by using CD. In Fig. 3*C*, small differences are observed in the CD spectra below 220 nm between a curve of the experimental mixture of the SH3 domain and Hsp47 and the theoretical curve created by addition of the individual curves of the SH3 domain and Hsp47. These differences are likely the result of small structural changes occurring from the interaction between the SH3 domain and Hsp47.

Hsp47 and a collagen model peptide were cocrystallized, and the binding region between Hsp47 and a triple helix was solved (23). The SH3 domain cannot share the binding site of Hsp47 with collagen if Hsp47 is an anchor molecule between TANGO1 and collagen. To evaluate the binding orientation among collagens, the SH3 domain, and Hsp47, SPR was performed by using immobilized type I collagen. Fig. 3*D* shows that the binding of the SH3 domain to Hsp47 is not competitive with the binding of Hsp47 to collagen. Moreover, because there is increased binding of the experimental mixture compared with the theoretical curve in Fig. 3*D*, binding of the SH3 domain to Hsp47 must occur at a different site than the Hsp47 collagen binding site. Therefore, Hsp47 can function as an anchor molecule between the SH3 domain of TANGO1 and collagens.

Does the Collagen Secretion Model Apply to Other Large ECM Molecules? The SH3 domain of TANGO1 showed binding to type VII collagen (11). In contrast to direct binding of the SH3 domain to collagens, we are proposing a global recognition model of the SH3 domain for collagen via Hsp47. It is possible that the special COPII vesicles for collagens may also be used by other ECM proteins because of their relatively large molecular size. Furthermore, COMP, a large pentameric molecule, was

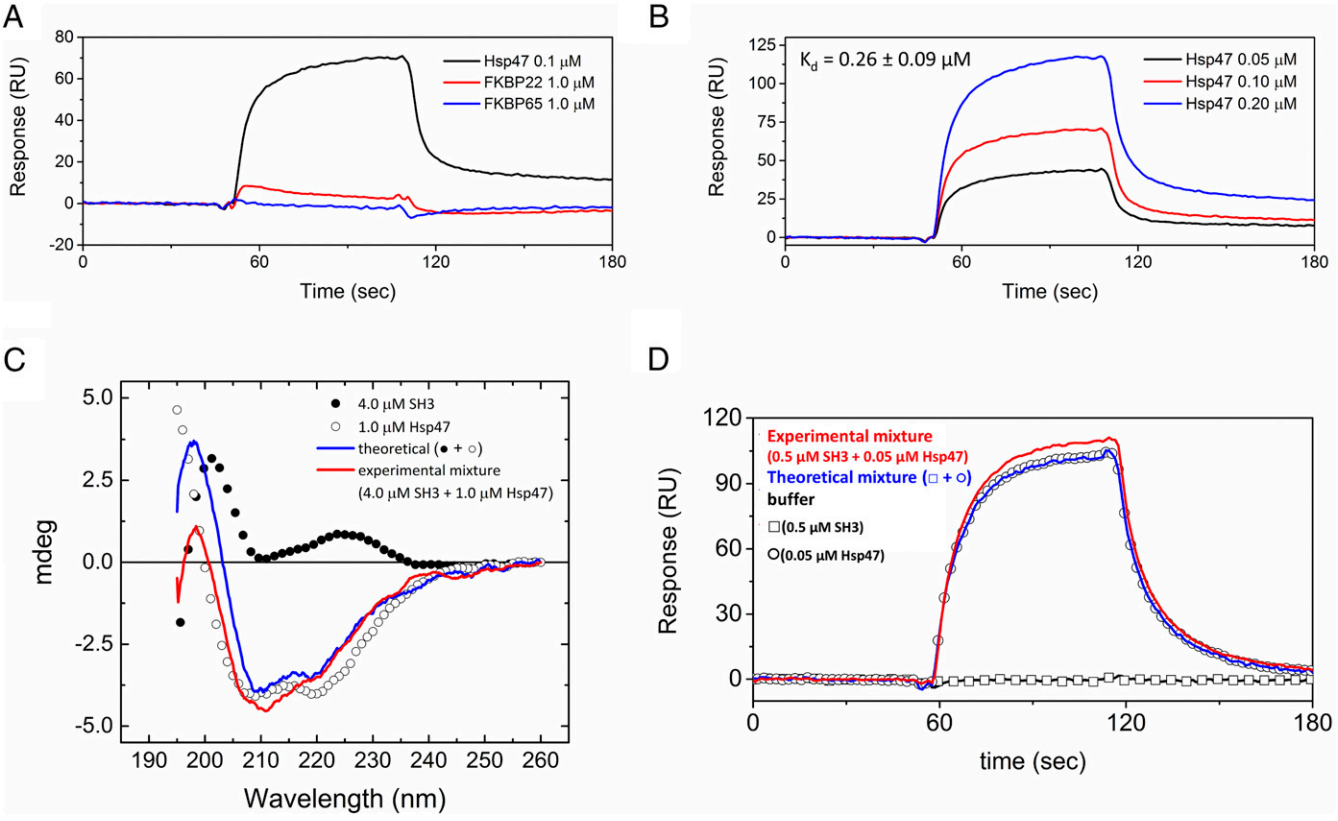

Fig. 3. Determination of the direct binding between the SH3 domain of human TANGO1 and Hsp47. (*A*) SPR analysis was carried out by using a BIAcore X instrument. Hsp47 (0.1 μM; black), FKBP22 (1.0 μM; red), and FKBP65 (1.0 μM; blue) were run over the CM5 chip with immobilized SH3 domain of human TANGO1. (*B*) Various concentrations of Hsp47 were run over the SH3 domain of human TANGO1 chip. The following binding curves are shown: 0.05 μM (black), 0.1 μM (red), and 0.2 μM (blue) Hsp47. The calculated K_d value is also shown. (*C*) CD spectra were measured at 4 °C in 10 mM phosphate, pH 7.5 The filled and open circles are the SH3 domain of human TANGO1 (4.0 μM) and Hsp47 (1.0 μM), respectively. Red and blue curves indicate the theoretical signal derived from addition of individual SH3 domain of human TANGO1 and Hsp47 signals, and the experimental signal from a mixture of the SH3 domain of human TANGO1 and Hsp47, respectively. (*D*) SPR analysis was carried out by using a BIAcore X instrument to determine the binding orientation. The open squares and circles are the SH3 domain of human TANGO1 (0.5 μM) and Hsp47 (0.05 μM), respectively. HBS-P buffer (10 mM Hepes buffer, pH 7.4, containing 150 mM NaCl, 1 mM $CaCl_2$, and 0.005% surfactant P20) is shown as a black curve. Red and blue curves indicate the theoretical signal derived from addition of individual SH3 domain of human TANGO1 and Hsp47 signals and the experimental signal from a mixture of both SH3 domain of human TANGO1 and Hsp47, respectively.

shown to form aggregates within the rER of TANGO1 KO chondrocytes (17). To test whether the SH3 domain and/or Hsp47 directly bind to larger ECM molecules, SPR experiments were carried out by using immobilized ECM molecules. COMP, fibronectin, and the amino- and carboxyl-terminal fragments of fibrillin-1, rF11, and rF6 (Fig. 4*E* shows a sketch of fibrillin-1 fragments) were coupled to CM5 sensor chips. The SH3 domain and/or Hsp47 were tested as analytes. Antibodies were used as a positive control. Binding of the SH3 domain of TANGO1 to these large ECM molecules was less than the weak binding to collagens (Fig. 4 *A*–*D* vs. Fig. 2). Although fibronectin and COMP were not directly recognized (Fig. 4 *A* and *B*), Hsp47 bound to fibrillin-1 and specifically interacted with rF11, but not rF6, in a concentration-dependent manner (Fig. 4 *C*, *D*, and *F*). However, the orientation of binding among the SH3 domain, Hsp47, and rF11 could not be clearly determined by SPR, in contrast to the case with collagens (Figs. 3*D* and 4*G*).

Is Fibrillin-1 a Novel Target of Hsp47 in the rER? According to the literature, Hsp47 is a collagen-specific molecular chaperone (24). From our SPR results (Fig. 4 *C* and *F*), we propose that Hsp47 may be involved in the biosynthesis, secretion, and/or quality control of fibrillin-1 in the rER. To evaluate the effects of Hsp47 on fibrillin-1, immunofluorescence staining experiments were performed by using Hsp47$^{+/+}$ and Hsp47$^{-/-}$ mouse embryonic fibroblasts (MEFs). Fig. 5*A* shows the presence of Hsp47 in Hsp47$^{+/+}$ MEFs, but not in Hsp47$^{-/-}$ MEFs. As previously reported (25), type I collagen was retained inside the cells of Hsp47$^{-/-}$ MEFs (Fig. 5*C*). Fibronectin networks were interestingly altered in Hsp47$^{-/-}$ MEFs. Fibronectin fibrils were thinner and shorter than in Hsp47$^{+/+}$ MEFs, but fibronectin did not appear to be retained inside the Hsp47$^{-/-}$ cells (Fig. 5*B*). In Hsp47$^{+/+}$ MEFs, the growth of fibrillin-1 microfibrils and type I collagen fibrils was observed (from thin and short to thick and short and then to thick and long; Figs. 5*C* and 6*A*). However, fibrillin-1 in Hsp47$^{-/-}$ MEFs surprisingly did not form these growing networks of fibrils. Instead, some dot-like staining appeared at day 7 (Fig. 6*A*). To determine whether the secretion of fibrillin-1 was normal, the amount of secreted fibrillin-1 was quantified by Western blotting by using the medium from equal numbers of Hsp47$^{+/+}$ and Hsp47$^{-/-}$ MEFs. Fig. 6*B* shows that similar amounts of secreted fibrilin-1 are present in Hsp47$^{+/+}$ and Hsp47$^{-/-}$ MEFs. Fig. 6*C* shows blotting against GAPDH (as a loading control) and Hsp47 and demonstrates that Hsp47$^{-/-}$ MEFs clearly lacked Hsp47.

Discussion

The Molecular Chaperone Hsp47 Is a Guide Molecule to Direct Collagens Toward Special Transport Vesicles in the rER. Hsp47 was first identified as a novel Hsp that interacts with collagen (26). It is now appreciated as the rER-resident collagen-specific molecular

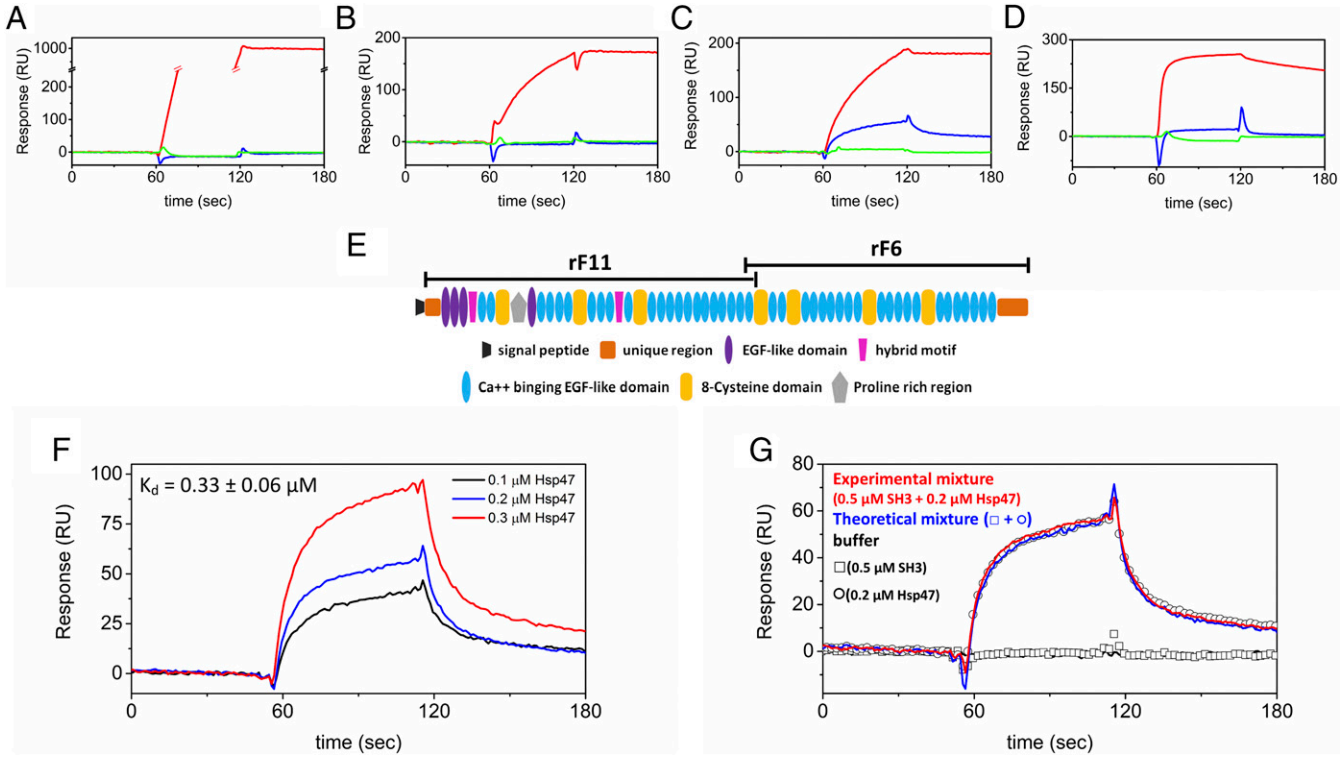

Fig. 4. Direct binding kinetics of Hsp47 to ECM molecules. Direct binding kinetics were measured by SPR analysis using a BIAcore X instrument. Antibodies against each ECM protein (red) were used as a positive control. Hsp47 (blue) and the SH3 domain of human TANGO1 (green) were injected over CM5 chips with immobilized ECM proteins. (*A*) Human fibronectin chip with 20 μg/mL anti-fibronectin, 0.8 μM Hsp47, and 10 μM SH3 domain of human TANGO1. (*B*) Human COMP chip with 40 μg/mL anti-COMP, 0.8 μM Hsp47, and 10 μM SH3 domain of human TANGO1. (*C*) Recombinant amino terminal fragment of human fibrillin-1 rF11 chip with 86 μg/mL anti-rF11, 0.2 μM Hsp47, and 10 μM SH3 domain of human TANGO1. (*D*) Recombinant carboxyl terminal fragment of human fibrillin-1 rF6 chip with 0.36 mg/mL anti-rF6, 0.8 μM Hsp47, and 10 μM SH3 domain of human TANGO1. (*E*) Domain structure of fibrillin-1 describing the fragments rF11 and rF6. (*F*) Various concentrations of Hsp47 were run over the recombinant amino-terminal fragment of human fibrillin-1 rF11 chip. The following binding curves are shown: 0.1 μM (black), 0.2 μM (red), and 0.3 μM (blue) Hsp47. The calculated K_d value is also shown. (*G*) SPR analysis was carried out by using a BIAcore X instrument to determine the binding orientation. The open squares and circles are the SH3 domain of human TANGO1 (0.5 μM) and Hsp47 (0.2 μM), respectively. HBS-P buffer (10 mM Hepes buffer, pH 7.4, containing 150 mM NaCl, 1 mM $CaCl_2$, and 0.005% Surfactant P20) is shown as a black curve. Red and blue curves indicate the theoretical signal derived from the addition of individual SH3 domain of human TANGO1 and Hsp47 signals and the experimental signal from a mixture of SH3 domain of human TANGO1 and Hsp47, respectively.

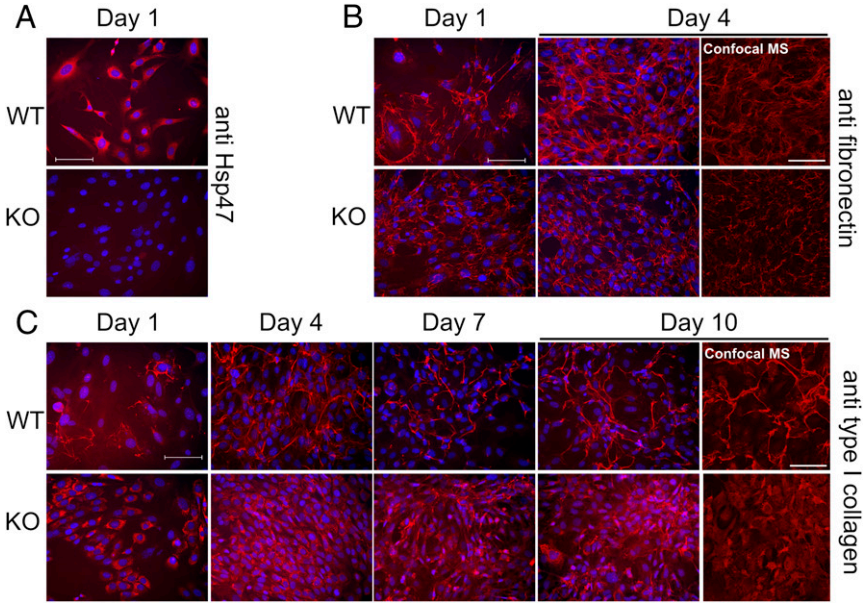

Fig. 5. Immunofluorescence staining in Hsp47$^{+/+}$ and Hsp47$^{-/-}$ MEFs. Hsp47$^{+/+}$ and Hsp47$^{-/-}$ MEFs were stained against anti-Hsp47 (*A*), anti-fibronectin (*B*), and anti-type I collagen (*C*). Cells were cultured with ascorbic acid phosphate (150 μg /mL) continuously, and fixed/permeabilized with cold methanol before staining was performed. The red and blue staining is derived from specific primary antibody and DAPI, respectively. Confocal images are included for day 4 of anti-fibronectin and day 10 of anti-type I collagen. These images are labeled as "confocal MS." (Scale bars: 100 μm.)

chaperone (24). The interaction between Hsp47 and collagens has been well characterized by biochemical, structural, and cell-biology approaches. Hsp47 recognizes the triple helical structure via Yaa-Gly-Xaa-Arg-Gly sequences with high–low affinity sites, depending on the amino acids in the Yaa position (27). All types of collagens possess at least multiple middle-affinity 4Hyp/Ser/Val/Ala-Gly-Xaa-Arg-Gly sequences, even if they do not have the high-affinity Thr-Gly-Xaa-Arg-Gly sequence (28). Hsp47 is also proposed to stabilize the triple helix in the rER (29). Moreover, the Hsp47 KO mouse is embryonic-lethal (30), and human and dachshund mutations in *SERPINH1*, coding for Hsp47, cause recessive osteogenesis imperfecta (OI) (31, 32). In all cases, a delay of type I collagen secretion and accumulation of type I collagen inside of cells is observed (table 2 in ref. 33).

Here, we propose a role for Hsp47 whereby it interacts with the SH3 domain of TANGO1 and performs as an anchor between TANGO1 and collagens. The binding affinity between the SH3 domain and Hsp47 ($K_d = 0.26 \pm 0.09$ μM; Fig. 3*B*) is comparable to that between collagen and Hsp47 ($K_d = 0.2$~4 μM) (20, 21). This indicates that these three molecules (i.e., collagen–Hsp47–SH3 domain) likely form an equilibrium complex at the rER exit site. We propose that the function of Hsp47 and TANGO1 is the loading and sorting of collagen molecules at the ER exit site.

The absence of Hsp47, or mutations in Hsp47, should exert a negative influence on directing collagens to the secretory pathway, as TANGO1 itself barely recognizes collagens. Similarly, the Hsp47–collagen complex should not be directed to special COPII vesicles in the absence of TANGO1. However, the physiological role of TANGO1 in type I collagen secretion became somewhat controversial because of cell biological studies with TANGO1 KO and knockdown experiments. Type I collagen secretion was affected in the TANGO1 KO cells, whereas it was not affected by the knockdown. In both cases, type VII collagen showed defective secretion (11, 15, 17). We hypothesize that the SH3 domain may interact more tightly with the large non-collagenous domain of type VII collagen, as our data show that the SH3 domain interacts only weakly with triple helical structures (Fig. 2). Although other mechanisms might exist to explain the molecular recognition of type VII collagen by the SH3 domain, it is clear that TANGO1 plays an important role in the secretion of collagens in vivo (17).

The mutations in human (L78P) and dachshund (L326P) Hsp47 lead to OI, and these mutant proteins show low expression levels and low binding to collagen and are unstable in cells (34). According to the crystal structure, these mutations are located on the opposite side of the collagen binding region (23). We hypothesize that the binding between Hsp47 and the SH3 domain occurs near these mutation sites and that the mutations alter regional structure, abolishing the interaction between Hsp47 and the SH3 domain and resulting in defective collagen secretion. Further studies are required to address the particular details of the interaction between Hsp47 and the SH3 domain of TANGO1. It is interesting to note that null mouse models of Hsp47, FKBP65, Prolyl 3-hydroxylase 1, and cartilage-associated protein show embryonic lethality or disturbances in various tissues (30, 35–37) and that human mutations in these proteins lead to a phenotype of recessive OI (38).

How Large ECM Molecules Are Sorted into Special COPII Transport Vesicles at the ER Exit Site Remains a Mystery. The SH3 domain of TANGO1 and/or the SH3–Hsp47 complex plays significant roles in collagen secretion. However, there are many other large secreted molecules. We selected fibronectin, COMP, and fibrillin-1 to determine whether the collagen secretion model is shared by these large ECM molecules. We found that fibronectin does not bind to the SH3 domain of TANGO1, nor to Hsp47 (Fig. 4*A*), consistent with the study with TANGO1 KO cells that showed that fibronectin secreted into the extracellular space (17). Therefore, there must be other mechanisms for the molecular sorting of fibronectin to special transport vesicles.

Type IX collagen is one of the binding partners of COMP (39), and COMP and type IX collagen are intracellularly retained by mutant COMP in pseudoachondroplasia chondrocytes (40–42). Interestingly, type IX collagen and COMP were also retained inside of TANGO1 KO cells (17). However, we found that COMP did not interact with the SH3 domain of TANGO1, nor with Hsp47 (Fig. 4*A*). It is possible that type IX collagen is required for COMP secretion and that Hsp47 loads type IX collagen–COMP complexes

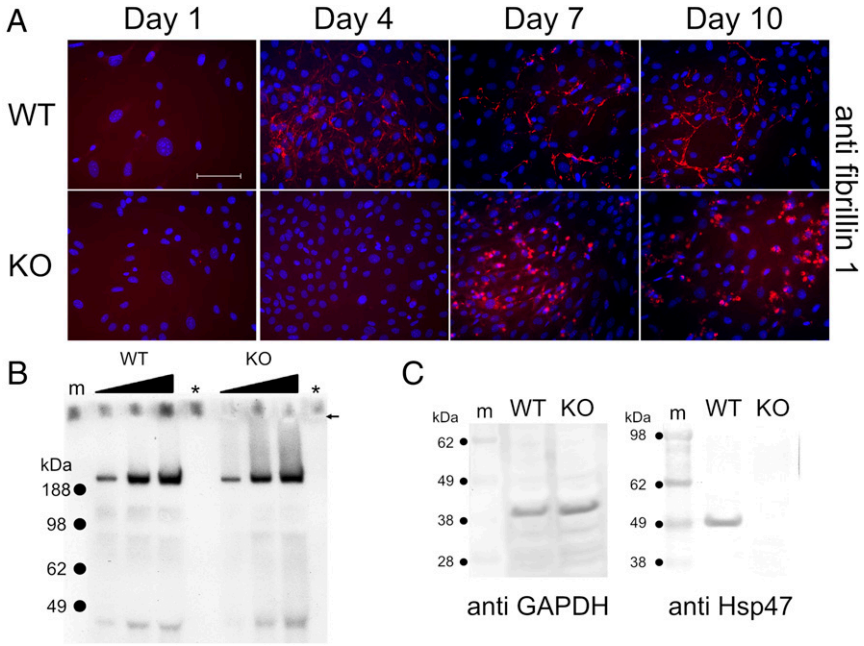

Fig. 6. Analysis of fibrillin-1 in Hsp47$^{+/+}$ and Hsp47$^{-/-}$ MEFs. (*A*) Hsp47$^{+/+}$ and Hsp47$^{-/-}$ MEFs were stained with anti–fibrillin-1. Cells were cultured with ascorbic acid phosphate (150 μg/mL) continuously and fixed/permeabilized with cold methanol before staining. The red and blue stainings are derived from specific primary antibody and DAPI, respectively. (Scale bar: 100 μm.) (*B*) Secreted amounts of fibrillin-1 in the serum-free medium from equal cell numbers were analyzed by Western blotting against fibrillin-1. The filled triangle and arrow indicate loading amounts on the well and well bottom, respectively. Blank and marker lanes are shown as asterisk and "m", respectively. (*C*) Total soluble proteins from equal cell numbers in Hsp47$^{+/+}$ and Hsp47$^{-/-}$ MEFs were extracted and blotted by using anti-GAPDH and anti-Hsp47. Marker is indicated as "m."

into special COPII vesicles via binding to the SH3 domain of TANGO1. Further studies are needed to understand the mechanism for cotrafficking of type IX collagen and COMP.

We expected that fibrillin-1 might share the same molecular sorting mechanism with collagens because of its interaction with Hsp47 (K_d = 0.33 ± 0.06 μM; Fig. 4*F*) showing similar binding affinity as collagen–Hsp47 (K_d = 0.2 ∼4 μM) (20, 21). However, fibrillin-1 was secreted normally into the medium of Hsp47$^{-/-}$ MEFs (Fig. 6*B*). Moreover, the competitive SPR experiment did not show the same results as for collagen (Figs. 3*D* and 4*G*), indicating that an SH3–Hsp47 complex does not interact with fibrillin-1. Therefore, fibrillin-1 likely has another trafficking pathway. Fibrillin-1 contains *N*-linked glycosaminoglycan side chains (43–45) and calcium-binding EGF-like domains (46–48). *N*-linked glycosylation and calcium binding occur in the rER (49, 50). The possibility that quality control is perturbed in the absence of Hsp47 is supported by our finding that microfibril formation by fibrillin-1 is abnormal in Hsp47$^{-/-}$ MEFs, even though secretion of fibrillin-1 appeared to be normal (Fig. 6). Further studies are required to understand the reason for the interaction of Hsp47 with fibrillin-1 in the rER.

We observed that the lack of Hsp47 disrupts matrix organization of type I collagen, fibronectin, and fibrillin-1 in Hsp47$^{-/-}$ MEFs (Figs. 5 and 6). Type I collagen was retained inside the cells of Hsp47$^{-/-}$ MEFs (Fig. 5*C*), as previously reported (25). In contrast to type I collagen, the secretion of fibronectin (25) and of fibrillin-1 was not affected by the absence of Hsp47 (Fig. 6*B*). However, the fibronectin network and microfibril formation by fibrillin-1 are affected in the Hsp47$^{-/-}$ MEFs cells (Figs. 5*B* and 6*A*). Because Hsp47 does not interact directly with fibronectin, it is possible that the observed defects in matrix organization are not caused directly by Hsp47.

Mature ECM networks develop properly in tissues only with the correct composition and quality of ECM proteins. If this balance is altered by mutations in a single gene for an ECM protein, there are consequences on matrix organization because the connective tissue is designed to hang together. Therefore, it is possible that disruption of the collagen fibril network caused by the absence of Hsp47 results in the observed differences in fibronectin and fibrillin-1 deposition and matrix organization. Future studies are required to determine if the difference in fibrillin-1 matrix organization is a result of necessary direct interactions of Hsp47 with fibrillin-1 in the rER or is indirectly caused by effects on collagen deposition and organization.

Conclusion

Here we describe an interaction between Hsp47 and the SH3 domain of TANGO1 and show that Hsp47 anchors the SH3 domain of TANGO1 to collagens. We propose that collagen molecules are directed into special COPII vesicles through complex formation between the SH3 domain of TANGO1 and Hsp47 at exit sites in the rER. This proposal is elegant because it can be applied to secretion of all types of collagens, and it provides the simplest explanation for observations gained from study of the TANGO1 KO mouse. As discussed, COMP may be retained by TANGO1 KO cells not because COMP uses the Hsp47–SH3 domain exit strategy, but because its type IX binding partner does use this exit strategy.

When we tried to test our model of collagen secretion by using other large ECM molecules, we were not able to show that it applies to COMP, fibronectin, or fibrillin-1. Although we may have uncovered a new role for Hsp47 in quality control of fibrillin-1, further studies are required to determine the precise function of Hsp47 interactions with fibrillin-1. Additional studies are also required to identify the mechanisms of molecular sorting and/or loading at the ER exit site for secretion of fibrillin-1 as well as for other large ECM molecules such as fibronectin. A summary of our model and hypotheses is shown in Fig. 7.

Materials and Methods

Expression and Purification of Recombinant SH3 Domain of Human TANGO1. The amino-terminal part of human TANGO1 cDNA (AK307412) was obtained from National Institute of Technology and Evaluation Biological Resource

Center (Chiba, Japan), and DNA encoding the SH3 domain of human TANGO1 (residues 1–106 of matured protein) was isolated by using this cDNA as the template by PCR using primers containing an EcoRI site at the 5′ end and a XhoI site after the stop codon at the 3′ end. That DNA was inserted between the EcoRI and XhoI restriction sites of a pET30a(+) expression vector (Invitrogen). The expression vectors were transformed into *E. coli* BL21(DE3) and grown at 37 °C to an optical density of 0.6 at 600 nm, and expression was induced with 1 mM isopropyl 1-thio-β-D-galactopyranoside. After incubation at 20 °C overnight, the cells were harvested by centrifugation and resuspended in Tris·base B-PER (Thermo Scientific) containing 1 mM $CaCl_2$. Insoluble material was removed by centrifugation, and proteins in the soluble fraction were precipitated with ammonium sulfate at a final concentration of 10% (wt/vol). After 2 h incubation at 4 °C, the sample was centrifuged, and the supernatant fraction was passed through a 0.22-μm filter and loaded onto a Co^{2+}-chelating column. After washing with 20 mM Hepes buffer, pH 7.5, containing 1.0 M NaCl, 1.0 M urea, 25 mM imidazole, and 1 mM $CaCl_2$ (minimum of five column volumes), the SH3 domain was eluted with elution buffer (20 mM Hepes buffer, pH 7.5, containing 1.0 M NaCl, 1.0 M urea, 500 mM imidazole, and 1 mM $CaCl_2$). The fractions containing the SH3 domain were dialyzed into enterokinase cleavage buffer (50 mM Tris·HCl buffer, pH 8.0, containing 1 mM $CaCl_2$ and 0.1% Tween 20). Enterokinase (1 U/mL reaction volume; Life Technology) was used to cleave the His tag at 4 °C overnight, and the sample was dialyzed into the washing buffer of the chelating column. The protein solution, including the SH3 domain, was treated with 1 μL/mL diisopropyl fluorophosphates to inactivate proteases derived from *E. coli* and gently stirred for 4 h on ice. This solution was applied onto a Co^{2+}-chelating column to remove the cleaved His tag fragment. The SH3 domain passed through the Co^{2+}-chelating column, and the flow-through fraction was dialyzed against 20 mM triethanolamine·HCl buffer, pH 7.5, containing 20 mM NaCl, 0.5 M urea, and 1 mM $CaCl_2$, loaded onto a HiTrap Q XL column (GE Healthcare), and washed with the same buffer (minimum of five column volumes). The contaminating proteins and the SH3 domain were eluted with 30% and 50% 20 mM triethanolamine·HCl buffer, pH 7.5, containing 500 mM NaCl, 0.5 M urea, and 1 mM $CaCl_2$, respectively. The purified SH3 domain was then dialyzed against different reaction buffers to remove urea and used for further experiments.

CD Measurements. CD spectra were recorded on an AVIV 202 spectropolarimeter (AVIV Biomedical) using a Peltier thermostated cell holder and a 1-mm path length rectangular quartz cell (Starna Cells). Protein concentrations were determined by amino acid analysis. The wavelength scanning experiments were done at 4 °C. The spectra represent the average of at least 10 scans recorded at a wavelength resolution of 0.1 nm. The temperature scanning experiments were measured at 10 °C/h. The ellipticity at 210 nm

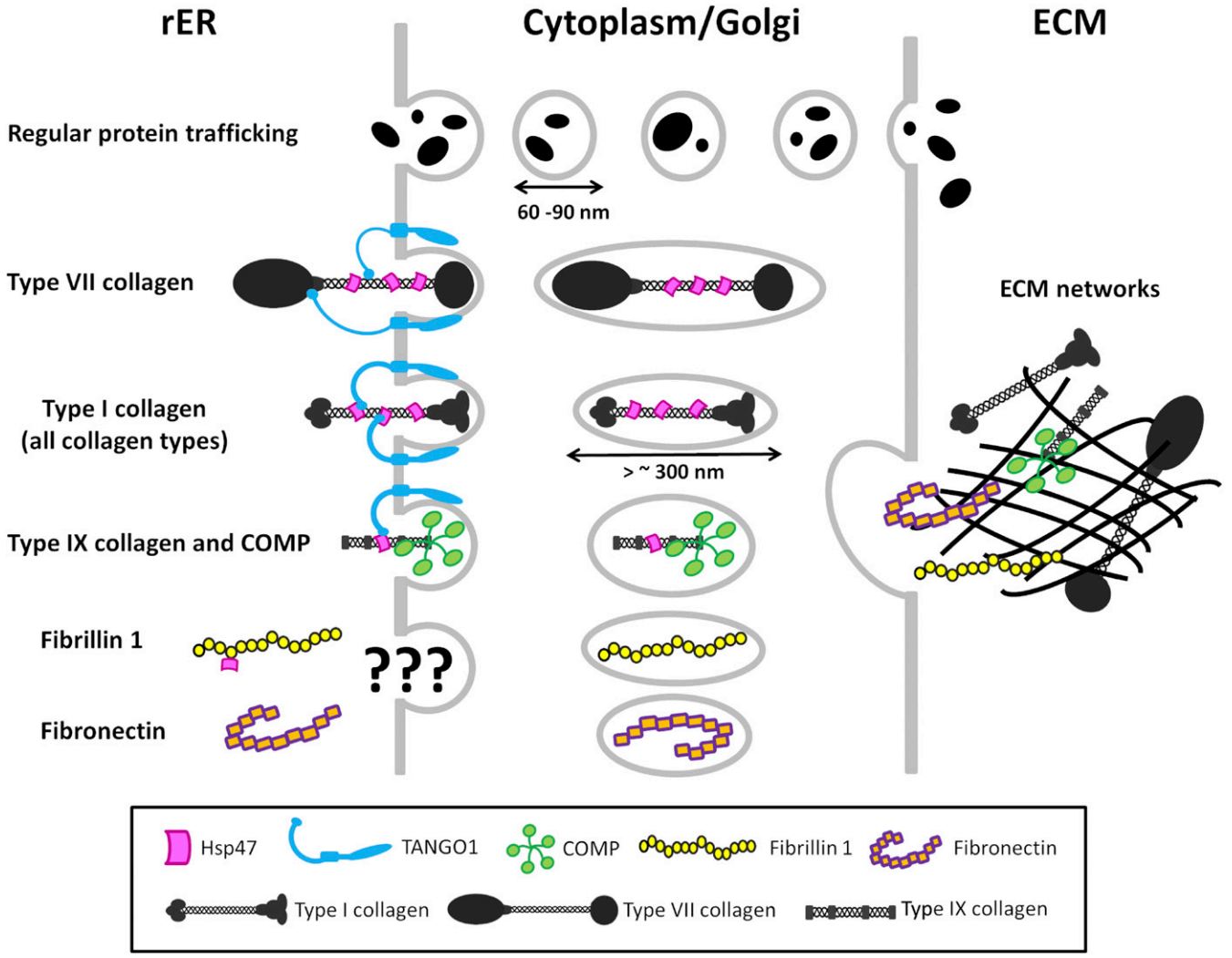

Fig. 7. Schematic diagram of the model and hypotheses for secretion of large ECM molecules. Type VII collagen is directed to special COPII vesicles by the SH3 domain of TANGO1 and by the SH3 domain–Hsp47 complex. All collagen types (type I collagen is shown in the model) are sorted and loaded into special COPII vesicles by the SH3 domain–Hsp47 complex. Type IX collagen may traffic to the extracellular space with COMP. Fibronectin and fibrillin-1 must be sorted into special COPII vesicles, but the SH3 domain–Hsp47 complex is not the mechanism of molecular recognition. The function of Hsp47 interaction with fibrillin-1 in the rER is unknown. Further investigations should be directed toward molecular mechanisms by which fibrillin-1 and fibronectin are sorted into special COPII vesicles and to the effects of mutations in Hsp47 (or loss of Hsp47) on matrix organization.

was monitored as a function of time. The proteins were measured in 10 mM phosphate, pH 7.5, and PBS solution for wavelength and temperature scanning experiment, respectively.

Preparation of Molecular Chaperones, Hsp47, FKBP22, and FKBP65. Hsp47 and FKBP65 were purified from 17-d-old chicken embryos with the methods described previously (51, 52). Human recombinant FKBP22 was purified from *E. coli* by methods described previously (20).

Preparation of Collagens and ECM Proteins. Isolation and purification of bovine type I, II, III, and V were described previously (20). Mouse type IV collagen and human recombinant type X collagen were purified as described by using HR9 and 293 cells, respectively (53, 54). Bovine type XI collagen was purified by the method described previously (55). The amino and carboxyl terminal fragments of human fibrillin 1, rF11, and rF6 were recombinantly expressed and characterized as described previously (56). Human fibronectin was purchased from R&D Systems. Human type VI collagen and COMP were provided by Takako Sasaki, Department of Biochemistry II, Faculty of Medicine, Oita University, Oita, Japan and Paul Holden, Department of Orthopedics and Rehabilitation, Oregon Health and Science University, respectively. Human tissue was obtained without patient identifiers and with ethical approval from the institutional review board at Oregon Health & Science University (Portland, OR).

SPR Analysis. SPR experiments were carried out using a BIAcore X instrument (GE Healthcare). Purified collagens, the SH3 domain of TANGO1 and ECM proteins, were immobilized on CM5 sensor chips by amide coupling. The approximate coupled protein concentrations were 6.0 ng/mm^2 [6,000 response units (RU)] of type I collagen, 1.2 ng/mm^2 (1,200 RU) of type II collagen, 3.0 ng/mm^2 (3,000 RU) of type III collagen, 4.5 ng/mm^2 (4,500 RU) of type IV collagen, 2.0 ng/mm^2 (2,000 RU) of type V collagen, 4.5 ng/mm^2 (4,500 RU) of type VI collagen, 3.0 ng/mm^2 (3,000 RU) of type X collagen, 0.95 ng/mm^2 (950 RU) of type XI collagen, 0.5 ng/mm^2 (500 RU) of SH3 domain of human TANGO1, 1.8 ng/mm^2 (1,800 RU) of fibronectin, 0.2 ng/mm^2 (200 RU) of COMP, 4.0 ng/mm^2 (4,000 RU) of rF11, and 2.3 ng/mm^2 (2,300 RU) of rF6. The experiments were performed at a flow rate of 10 μL/min and 20 °C in HBS-P buffer (10 mM Hepes buffer, pH 7.4, containing 150 mM NaCl, 1 mM $CaCl_2$, and 0.005% Surfactant P20). All curves are the average of at least three replicates for three independent measurements. For analysis of binding affinity, the curves were fitted with the Langmuir binding model (BIAevaluation software; GE Healthcare).

Antibodies. Mouse monoclonal antibody against Hsp47 (ADI-SPA-470; Enzo Life Sciences), sheep polyclonal antibody against fibronectin (AF1918; R&D Systems), rabbit polyclonal antibody against mouse type I collagen (AB765P; EMD Millipore), goat polyclonal antibody against COMP (AF3134; R&D Systems), and rabbit polyclonal antibody against GAPDH (PLA0125; Sigma-Aldrich) were obtained from the indicated sources. Antibodies against rF11 (polyclonal antibody 9543) and rF6 (monoclonal antibody 69) were generated with recombinant peptides and characterized as described previously (56). Alexa Fluor 568-conjugated anti-mouse and anti-rabbit IgG (A-11019 and A-21069; Thermo Fisher Scientific) and NorthernLights NL557 conjugated anti sheep IgG (NL010; R&D Systems) were used as secondary antibodies for immunofluorescence staining. Alkaline phosphatase-conjugated anti-mouse and anti-rabbit IgG and HRP-conjugated anti-rabbit IgG (A5781, A9919, and A2304; Sigma-Aldrich) were used as secondary antibodies for Western blotting.

Cell Culture. Hsp47$^{+/+}$ and Hsp47$^{-/-}$ MEFs were cultured in DMEM with 4.5 g/L glucose, L-glutamine, and sodium pyruvate containing 10% (vol/vol) FBS (Atlanta Biologicals), Pen Strep Glutamine (100×; Life Technology), and 5 mM Hepes in presence of ascorbic acid phosphate (150 μg/mL; Wako Chemicals).

Immunofluorescence Staining. An equal number of cells (100,000 cells per milliliter) of Hsp47$^{+/+}$ and Hsp47$^{-/-}$ MEFs were grown in a Nunc Lab-Tek Chamber Slide System (Thermo Fisher Scientific) under the same condition as described earlier. The cells were cultured at each time point (days 1, 4, 7, and 10), washed in PBS solution, and fixed/permeabilized with cold methanol for 10 min. After washing in PBS solution, the cells were incubated with specific antibodies at room temperature for 2 h. The dilution ratios of antibodies are: 1:50 for anti-Hsp47, 1:20 for fibronectin, 1:40 for type I collagen, and 1:400 for fibrillin 1. After incubation with antibodies and washing in PBS solution, fluorophore-conjugated secondary antibodies were added to the cells at a 1:1,000 dilution in the dark for 30 min. After washing in PBS solution, a coverslip was placed with the aqueous mounting medium Fluoroshield with DAPI (Sigma-Aldrich) and stored in the dark overnight at room temperature. Immunofluorescence was observed with a Zeiss AxioVert 200 microscope with ApoTome, and micrographs were recorded digitally using the AxioVision software (version 4.6). Confocal images were collected on a TCS SP2 (Leica Microsystems) by using a Leica DMIRE2 inverted microscope with a 20× lens (0.7 NA) with the following imaging parameters: excitation 543 nm, scan speed of 200 lines per minute, 4× line average, and an image size of 1,024 × 1,024.

Western Blotting. An equal number of cells (300,000 cells per dish) of Hsp47$^{+/+}$ and Hsp47$^{-/-}$ MEFs were cultured in 100-mm dishes under the same condition as detailed earlier. The medium was replaced with serum-free medium after cells were fed with serum for 8 h, and cells were incubated overnight. Secreted proteins in the medium were precipitated with trichloroacetic acid and dissolved in NuPAGE LDS sample buffer (Life Technology) without reducing agents. Cell lysates were extracted using M-PER (Thermo Fisher Scientific) containing protease inhibitors at 4 °C. After centrifugation, soluble proteins in the extract were mixed with NuPAGE LDS sample buffer with reducing agents. These protein solutions were separated by NuPAGE Novex Bis-Tris 4–12% gel (Life Technology) and electrotransferred onto PVDF membranes. Antibodies were incubated to detect the specific protein after the membranes were blocked in PBS solution containing 5% (vol/vol) skim milk. Secreted fibrillin 1 was detected by HRP enhanced with SuperSignal West Pico Chemiluminescent Substrate (Thermo Fisher Scientific), and signals were exposed to Amersham Hyperfilm MP (GE Healthcare). GAPDH and Hsp47 in the cell lysate were detected by alkaline phosphatase developed with 5-bromo-4-chloro-3-indolyl phosphate and Nitro blue tetrazolium.

ACKNOWLEDGMENTS. We thank Dr. Takako Sasaki and Dr. Paul Holden for providing human type VI collagen and COMP. This study was supported by Shriners Hospital for Children Grants 85100 and 85500 (to H.P.B.) and 79135 (to L.Y.S.).

1. Bateman JF, Boot-Handford RP, Lamandé SR (2009) Genetic diseases of connective tissues: Cellular and extracellular effects of ECM mutations. *Nat Rev Genet* 10(3):173–183.
2. D'Arcangelo JG, Stahmer KR, Miller EA (2013) Vesicle-mediated export from the ER: COPII coat function and regulation. *Biochim Biophys Acta* 1833(11):2464–2472.
3. Miller EA, Schekman R (2013) COPII - A flexible vesicle formation system. *Curr Opin Cell Biol* 25(4):420–427.
4. Unlu G, Levic DS, Melville DB, Knapik EW (2014) Trafficking mechanisms of extracellular matrix macromolecules: Insights from vertebrate development and human diseases. *Int J Biochem Cell Biol* 47:57–67.
5. Bächinger HP, Mizuno K, Vranka J, Boudko S (2010) Collagen formation and structure. *Comprehensive Natural Products II: Chemistry and Biology*, eds Mander L, Liu HW (Elsevier, Amsterdam), pp 469–530.
6. Ricard-Blum S (2011) The collagen family. *Cold Spring Harb Perspect Biol* 3(1):a004978.
7. Sakai LY, Keene DR, Glanville RW, Bächinger HP (1991) Purification and partial characterization of fibrillin, a cysteine-rich structural component of connective tissue microfibrils. *J Biol Chem* 266(22):14763–14770.
8. Bonfanti L, et al. (1998) Procollagen traverses the Golgi stack without leaving the lumen of cisternae: Evidence for cisternal maturation. *Cell* 95(7):993–1003.
9. Malhotra V, Erlmann P (2015) The pathway of collagen secretion. *Annu Rev Cell Dev Biol* 31:109–124.
10. Saito K, Katada T (2015) Mechanisms for exporting large-sized cargoes from the endoplasmic reticulum. *Cell Mol Life Sci* 72(19):3709–3720.
11. Saito K, et al. (2009) TANGO1 facilitates cargo loading at endoplasmic reticulum exit sites. *Cell* 136(5):891–902.
12. Saito K, et al. (2011) cTAGE5 mediates collagen secretion through interaction with TANGO1 at endoplasmic reticulum exit sites. *Mol Biol Cell* 22(13):2301–2308.
13. Jin L, et al. (2012) Ubiquitin-dependent regulation of COPII coat size and function. *Nature* 482(7386):495–500.
14. Venditti R, et al. (2012) Sedlin controls the ER export of procollagen by regulating the Sar1 cycle. *Science* 337(6102):1668–1672.
15. Nogueira C, et al. (2014) SLY1 and Syntaxin 18 specify a distinct pathway for procollagen VII export from the endoplasmic reticulum. *eLife* 3:e02784.
16. Santos AJ, Raote I, Scarpa M, Brouwers N, Malhotra V (2015) TANGO1 recruits ERGIC membranes to the endoplasmic reticulum for procollagen export. *eLife* 4:4.
17. Wilson DG, et al. (2011) Global defects in collagen secretion in a Mia3/TANGO1 knockout mouse. *J Cell Biol* 193(5):935–951.
18. Harkiolaki M, et al. (2003) Structural basis for SH3 domain-mediated high-affinity binding between Mona/Gads and SLP-76. *EMBO J* 22(11):2571–2582.
19. Saksela K, Permi P (2012) SH3 domain ligand binding: What's the consensus and where's the specificity? *FEBS Lett* 586(17):2609–2614.
20. Ishikawa Y, Bächinger HP (2014) A substrate preference for the rough endoplasmic reticulum resident protein FKBP22 during collagen biosynthesis. *J Biol Chem* 289(26):18189–18201.
21. Natsume T, Koide T, Yokota S, Hirayoshi K, Nagata K (1994) Interactions between collagen-binding stress protein HSP47 and collagen. Analysis of kinetic parameters by surface plasmon resonance biosensor. *J Biol Chem* 269(49):31224–31228.

22. Ishikawa Y, Bächinger HP (2013) A molecular ensemble in the rER for procollagen maturation. *Biochim Biophys Acta* 1833(11):2479–2491.
23. Widmer C, et al. (2012) Molecular basis for the action of the collagen-specific chaperone Hsp47/SERPINH1 and its structure-specific client recognition. *Proc Natl Acad Sci USA* 109(33):13243–13247.
24. Ishida Y, Nagata K (2011) Hsp47 as a collagen-specific molecular chaperone. *Methods Enzymol* 499:167–182.
25. Ishida Y, et al. (2006) Type I collagen in Hsp47-null cells is aggregated in endoplasmic reticulum and deficient in N-propeptide processing and fibrillogenesis. *Mol Biol Cell* 17(5):2346–2355.
26. Nagata K, Saga S, Yamada KM (1986) A major collagen-binding protein of chick embryo fibroblasts is a novel heat shock protein. *J Cell Biol* 103(1):223–229.
27. Koide T, et al. (2006) Specific recognition of the collagen triple helix by chaperone HSP47: Minimal structural requirement and spatial molecular orientation. *J Biol Chem* 281(6):3432–3438.
28. Koide T, et al. (2006) Specific recognition of the collagen triple helix by chaperone HSP47. II. The HSP47-binding structural motif in collagens and related proteins. *J Biol Chem* 281(16):11177–11185.
29. Makareeva E, Leikin S (2007) Procollagen triple helix assembly: An unconventional chaperone-assisted folding paradigm. *PLoS One* 2(10):e1029.
30. Nagai N, et al. (2000) Embryonic lethality of molecular chaperone hsp47 knockout mice is associated with defects in collagen biosynthesis. *J Cell Biol* 150(6):1499–1506.
31. Drögemüller C, et al. (2009) A missense mutation in the SERPINH1 gene in Dachshunds with osteogenesis imperfecta. *PLoS Genet* 5(7):e1000579.
32. Christiansen HE, et al. (2010) Homozygosity for a missense mutation in SERPINH1, which encodes the collagen chaperone protein HSP47, results in severe recessive osteogenesis imperfecta. *Am J Hum Genet* 86(3):389–398.
33. Lindert U, et al. (2015) Molecular consequences of the SERPINH1/HSP47 mutation in the dachshund natural model of osteogenesis imperfecta. *J Biol Chem* 290(29): 17679–17689.
34. Ito S, Nagata K (2016) Mutants of collagen-specific molecular chaperone Hsp47 causing osteogenesis imperfecta are structurally unstable with weak binding affinity to collagen. *Biochem Biophys Res Commun* 469(3):437–442.
35. Lietman CD, et al. (2014) Connective tissue alterations in Fkbp10-/- mice. *Hum Mol Genet* 23(18):4822–4831.
36. Morello R, et al. (2006) CRTAP is required for prolyl 3- hydroxylation and mutations cause recessive osteogenesis imperfecta. *Cell* 127(2):291–304.
37. Vranka JA, et al. (2010) Prolyl 3-hydroxylase 1 null mice display abnormalities in fibrillar collagen-rich tissues such as tendons, skin, and bones. *J Biol Chem* 285(22): 17253–17262.
38. Marini JC, Reich A, Smith SM (2014) Osteogenesis imperfecta due to mutations in non-collagenous genes: Lessons in the biology of bone formation. *Curr Opin Pediatr* 26(4): 500–507.
39. Holden P, et al. (2001) Cartilage oligomeric matrix protein interacts with type IX collagen, and disruptions to these interactions identify a pathogenetic mechanism in a bone dysplasia family. *J Biol Chem* 276(8):6046–6055.
40. Maddox BK, et al. (1997) The fate of cartilage oligomeric matrix protein is determined by the cell type in the case of a novel mutation in pseudoachondroplasia. *J Biol Chem* 272(49):30993–30997.
41. Délot E, Brodie SG, King LM, Wilcox WR, Cohn DH (1998) Physiological and pathological secretion of cartilage oligomeric matrix protein by cells in culture. *J Biol Chem* 273(41):26692–26697.
42. Vranka J, et al. (2001) Selective intracellular retention of extracellular matrix proteins and chaperones associated with pseudoachondroplasia. *Matrix Biol* 20(7):439–450.
43. Ashworth JL, Kelly V, Rock MJ, Shuttleworth CA, Kielty CM (1999) Regulation of fibrillin carboxy-terminal furin processing by N-glycosylation, and association of amino- and carboxy-terminal sequences. *J Cell Sci* 112(Pt 22):4163–4171.
44. Maslen CL, Corson GM, Maddox BK, Glanville RW, Sakai LY (1991) Partial sequence of a candidate gene for the Marfan syndrome. *Nature* 352(6333):334–337.
45. Sakai LY, Keene DR, Engvall E (1986) Fibrillin, a new 350-kD glycoprotein, is a component of extracellular microfibrils. *J Cell Biol* 103(6 pt 1):2499–2509.
46. Corson GM, Chalberg SC, Dietz HC, Charbonneau NL, Sakai LY (1993) Fibrillin binds calcium and is coded by cDNAs that reveal a multidomain structure and alternatively spliced exons at the 5′ end. *Genomics* 17(2):476–484.
47. Reinhardt DP, et al. (1997) Calcium determines the shape of fibrillin. *J Biol Chem* 272(11):7368–7373.
48. Reinhardt DP, Ono RN, Sakai LY (1997) Calcium stabilizes fibrillin-1 against proteolytic degradation. *J Biol Chem* 272(2):1231–1236.
49. Lam AK, Galione A (2013) The endoplasmic reticulum and junctional membrane communication during calcium signaling. *Biochim Biophys Acta* 1833(11):2542–2559.
50. Aebi M (2013) N-linked protein glycosylation in the ER. *Biochim Biophys Acta* 1833(11):2430–2437.
51. Ishikawa Y, Vranka J, Wirz J, Nagata K, Bächinger HP (2008) The rough endoplasmic reticulum-resident FK506-binding protein FKBP65 is a molecular chaperone that interacts with collagens. *J Biol Chem* 283(46):31584–31590.
52. Macdonald JR, Bächinger HP (2001) HSP47 binds cooperatively to triple helical type I collagen but has little effect on the thermal stability or rate of refolding. *J Biol Chem* 276(27):25399–25403.
53. Wagner K, et al. (2000) Coexpression of alpha and beta subunits of prolyl 4-hydroxylase stabilizes the triple helix of recombinant human type X collagen. *Biochem J* 352(pt 3):907–911.
54. Davis JM, Boswell BA, Bächinger HP (1989) Thermal stability and folding of type IV procollagen and effect of peptidyl-prolyl cis-trans-isomerase on the folding of the triple helix. *J Biol Chem* 264(15):8956–8962.
55. Morris NP, Bächinger HP (1987) Type XI collagen is a heterotrimer with the composition (1 alpha, 2 alpha, 3 alpha) retaining non-triple-helical domains. *J Biol Chem* 262(23):11345–11350.
56. Reinhardt DP, et al. (1996) Fibrillin-1: Organization in microfibrils and structural properties. *J Mol Biol* 258(1):104–116.